Thermal resistance between crossed carbon nanotubes: Molecular dynamics simulations and analytical modeling

Guo-Jie Hu and Bing-Yang Cao[a)]
Key Laboratory for Thermal Science and Power Engineering of Ministry of Education, Department of Engineering Mechanics, Tsinghua University, Beijing 100084, People's Republic of China

(Received 16 August 2013; accepted 22 November 2013; published online 11 December 2013)

A nonequilibrium molecular dynamics (MD) method is used to calculate the thermal resistance between crossed carbon nanotubes (CNTs). The thermal resistance is predicted to be of the order of 10^9–10^{11} K/W. The effects of the crossing angle, nanotube length, and initial nanotube spacing on the thermal resistance are studied in detail with the fixed boundary condition applied in the axial direction of each CNT. The thermal resistance is found to increase with the increasing crossing angle while decrease with the increasing nanotube length and converge to a constant eventually. An increase in the thermal resistance is observed for nanotubes with larger initial spacing and the increase becomes abrupt as the initial spacing is increased to the van der Waals diameter. Between the crossed CNTs the phonon transport is constricted through the contact. The thermal resistance between the crossed CNTs calculated by MD is found to be close to the ballistic constriction resistance, which indicates that the constriction thermal resistance plays a major role in the inter-tube thermal resistance and the ballistic transport of phonons is dominant in the thermal transport between the crossed CNTs. © *2013 AIP Publishing LLC*. [http://dx.doi.org/10.1063/1.4842896]

I. INTRODUCTION

Carbon nanotubes (CNTs), including single-walled CNTs (SWNTs)[1,2] and multiwalled CNTs,[3,4] have been reported to show high thermal conductivities, which has stimulated great interest in their applications in the thermal management field. CNTs have been embedded into polymer composites,[5,6] dispersed in fluids,[7,8] and used to coat substrates[9] to improve the heat transport properties. However, the measured thermal conductivities of the CNT composites and suspensions are much lower than expected.[10] The thermal resistance between the CNTs and surrounding medium is believed to be a key factor hindering the heat flow.[11,12] Except for that the thermal resistance between CNTs is another important but less-studied factor impacting the effective thermal conductivity of CNTs-based materials. The bulk CNT samples, such as the CNT mats, films, arrays, and ropes, in which the CNTs often intermingle with each other giving rise to a significant number of CNT/CNT transverse interfaces, are explored to have much lower thermal conductivities than individual CNTs.[13,14] The reduction of the thermal conductivity arises from the thermal resistance at the interfaces formed between the CNTs. Thus, it is important to study the thermal resistance between CNTs so that the enhancement of the thermal conductivity in bulk CNT samples can be achieved and the CNT/CNT heat transfer process can be well understood.

The thermal resistance at an interface, also known as Kapitza resistance,[15] is defined as

$$R = \frac{\Delta T}{\dot{Q}}, \tag{1}$$

where $\dot{Q}$ and ΔT correspond to the heat flux across the interface and the associated temperature drop, respectively. The thermal resistance at a CNT/CNT interface has been investigated using various methods.[16–22] Table I lists the reported thermal resistance of CNT-CNT contacts along with their methodologies and structures. Maruyama *et al.*[16] simulated a non-stationary heat transfer process in a SWNT bundle using the MD method and obtained the thermal conductance between SWNTs in a bundle to be about 4.04 MW/m^2 K from which the thermal resistance could be estimated to be around 1.38×10^{10} K/W. Zhong and Lukes[17] studied the interfacial thermal transport between two offset parallel (10, 10) SWNTs with various configurations using MD simulations. They observed that the thermal resistance at the contact between parallel nanotubes depended on the nanotube spacing, overlap and length, and the increasing tube-tube contact dramatically reduced the interfacial resistance. Xu *et al.*[18] also investigated the parallel SWNTs and obtained the enhancement of the interfacial thermal conductivity by polymer wrapping at the interface between CNTs. Besides, Varshney *et al.*[19] considered the effect of the organic linkers connecting the CNTs on the thermal resistance at the interface. They explored the resistance between two parallel-bonded as well as nonbonded CNTs embedded in an epoxy matrix using MD simulations and found that the incorporation of linker molecules significantly modified the interfacial heat transfer. Recently, the junction conduction of crossed CNTs was also computed. Evans *et al.*[20] investigated the junction conduction as a function of crossing angle and pressure and presented an expression of the total junction resistance as the sum of the internal resistance associated with moving heat from high frequency modes in nanotube to low frequency modes and the external resistance associated with

a)Author to whom correspondence should be addressed. Electronic mail: caoby@tsinghua.edu.cn. Tel./Fax: 86-10-6279-4531.

 © 2013 AIP Publishing LLC

[This article is copyrighted as indicated in the article. Reuse of AIP content is subject to the terms at: http://scitation.aip.org/termsconditions. Downloaded to] IP: 101.6.32.33 On: Thu, 12 Dec 2013 00:34:47

TABLE I. Reported thermal resistance at CNT/CNT interfaces. All the values have been converted into unit of K/W.

Researcher	Method	Structure	CNT length (nm)	Thermal resistance (K/W)
Maruyama *et al.*[16]	MD simulations		2.51	1.38×10^{10}
Zhong and Lukes[17]	MD simulations	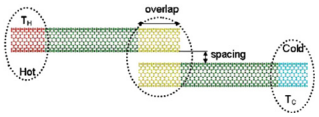	5	$6–7 \times 10^{10}$
Xu *et al.*[18]	MD simulations	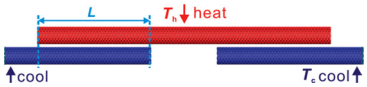	>10	$10^9–10^{10}$
Varshney *et al.*[19]	MD simulations	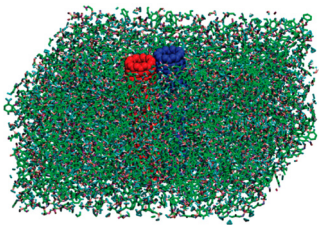	4.3	$2–5 \times 10^9$
Evans *et al.*[20]	MD simulations	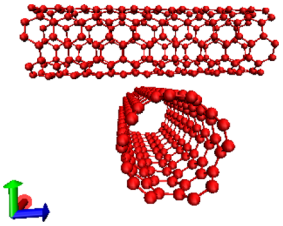	2	2.32×10^{10}
Yang *et al.*[22]	Experiments	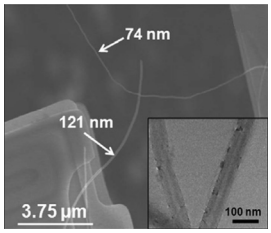	>2500	$\sim 1 \times 10^7$

heat flow between the tubes predominantly via low frequency modes. In order to model the two thermal resistances placed in series, they simply assumed the internal resistance proportional to the tube length and the external resistance proportional to the contact area. Except for these MD studies, some experimental researches and model-based analyses have also been carried out. Based on the measured thermal properties of bulk samples, Cola *et al.*[21] developed a contact resistance model to describe heat transfer across CNT array interfaces. Yang *et al.*[22] derived the thermal contact resistance from the measured total thermal resistance of two individual CNTs with a contact between them by subtracting the thermal resistance of the CNTs.

It can be seen that the thermal resistance at a CNT/CNT contact has been predicted but the mechanism of CNT/CNT thermal transport was not analyzed clearly. In the studies to date, the resistance was generally regarded as a thermal contact resistance and simply assumed to proportionally depend on the contact area and pressure. However, the mechanism of the thermal resistance is not clear and needs further investigation. Besides, how the configuration parameters influence the thermal resistance at CNT/CNT contacts was not studied comprehensively, especially for the contacts between crossed CNTs.

In this paper, the thermal resistances between the crossed SWNTs are investigated by using MD simulations and the effects of the crossing angle, nanotube length, and initial nanotube spacing on the thermal resistance are explored in detail. Further, based on a thermal constriction resistance model, the interfacial heat transfer mechanisms and the analytical modeling of the thermal resistance between the crossed CNTs are discussed.

II. SIMULATION METHOD

The nonequilibrium molecular dynamics (NEMD) method[23] is used here to simulate the interfacial heat transfer

[This article is copyrighted as indicated in the article. Reuse of AIP content is subject to the terms at: http://scitation.aip.org/termsconditions. Downloaded to] IP: 101.6.32.33 On: Thu, 12 Dec 2013 00:34:47

in a system of offset crossed CNTs. The general configuration in terms of crossing angle, nanotube length, and initial nanotube spacing is shown in Figure 1. The system consists three crossed (5, 5) SWNTs that are modeled with a C-C bond length of 0.144 nm.[24] The crossing angle refers to the angle between the axes of two neighboring tubes and is equivalent for each pair. The nanotube length denotes the equal length of each SWNT. The spacing is defined as the smallest distance between the outer walls of the neighboring nanotubes and is measured from the centers of the atoms in those walls. Besides, one ring of atoms at each end of each SWNT is fixed to prevent rotation and axial translation of the nanotubes.

The MD procedure involves an integration of Newton's classical equations of motion for atoms interacting with each other through an empirical interatomic potential. It is an atomistic model that simulates phonon-phonon interaction but ignores electron transport. As the phonon contribution to heat conduction is dominant in CNTs, the MD method is appropriate for the current problem. Based on the definition of the thermal resistance at an interface, the temperature drop and heat flux need to be calculated to determine the resistance. In our simulations, the temperatures of the first and third SWNTs along y direction (in Figure 1) are maintained at $T_L = T_0 - \delta T$ and $T_H = T_0 + \delta T$. Here, T_0 is the mean system temperature and δT is the difference between the heat bath

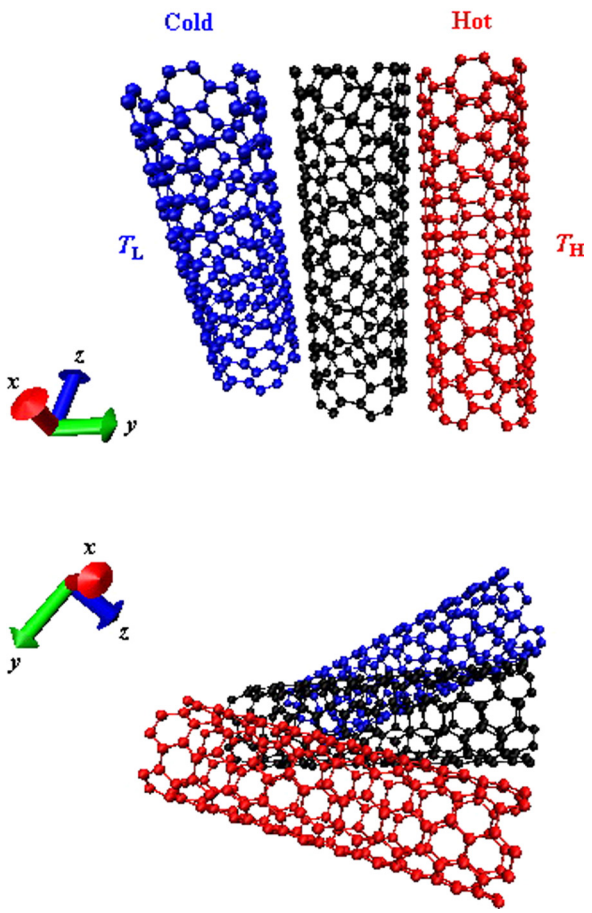

FIG. 1. The MD simulation system. Three SWNTs are configured with the crossing angle, initial nanotube spacing and nanotube length varied to see the effects on the thermal resistance at the CNT/CNT contacts.

temperature and T_0. The temperatures are maintained by the Nose-Hoover thermostat method.[25–27] Then, a nonequilibrium state is established in the system. To obtain the temperature profile of the nonequilibrium system, each SWNT is divided into 2 slabs along the transverse direction and the transient local temperature is calculated for each slab using equipartition,

$$T = \frac{1}{3nk_B}\sum_{i=1}^{n} m_i v_i^2, \tag{2}$$

where n is the number of atoms in the slab, k_B is Boltzmann's constant, m_i and v_i are the mass and velocity of atom i, respectively. From the temperature profile, the temperature drops at the interfaces between neighboring SWNTs as well as the temperature distribution of each SWNT along transverse direction can be determined.

The interactions between the carbon atoms include the intra-tube C-C bonded interactions and inter-tube van der Waals interactions. The C-C bonded interactions are modeled by the Brenner potential,[28]

$$E_b = \sum_i \sum_{j(>i)} \left[V_R(r_{ij}) - B_{ij} V_A(r_{ij})\right], \tag{3}$$

where E_b is the total C-C bond potential of the system, B_{ij} is the many-body interaction parameter which represents the many-body coupling between the bond from atom i to atom j and the local environment of atom i, V_R and V_A are the repulsive and attractive pair terms, and r_{ij} is the intermolecular distance between atom i and atom j. The inter-tube van der Waals interactions are based on the Lennard-Jones (LJ) potential,

$$V(r) = 4\varepsilon\left[\left(\frac{\sigma}{r}\right)^{12} - \left(\frac{\sigma}{r}\right)^{6}\right], \tag{4}$$

where r is the intermolecular distance, $\varepsilon = 2.968$ meV is the energy parameter, and $\sigma = 0.3407$ nm is the van der Waals diameter.[29]

The motion equations for the molecules are integrated using the Leap-Frog algorithm. Each case is run for 25 ps for equilibrating the system at the mean temperature which is set to 300 K and then for 250 ps to impose the heat baths on the corresponding SWNTs and stabilize the heat transfer. Here, δT is set to 30 K. After that, the local slab temperatures and heat flux are averaged over 2500 ps. This time length is sufficient to obtain converged results as shown below.

III. RESULTS AND DISCUSSION

A. MD simulation results

The temperature evolution for the system with a tube length of 1.25 nm, a crossing angle of 20° and an initial nanotube spacing of 0.5σ as a function of statistics time is shown in the inset in Figure 2. The statistics begins after imposing the heat bath and thus the temperature of the hot and cold SWNTs have been maintained at 330 K and 270 K,

[This article is copyrighted as indicated in the article. Reuse of AIP content is subject to the terms at: http://scitation.aip.org/termsconditions. Downloaded to] IP: 101.6.32.33 On: Thu, 12 Dec 2013 00:34:47

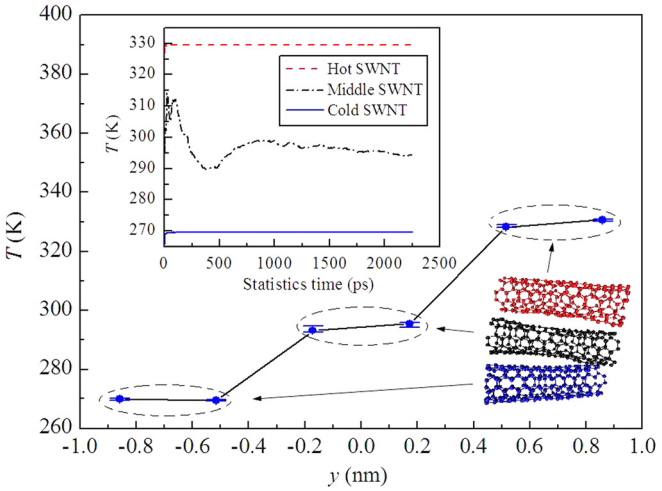

FIG. 2. Temperature profile and temperature evolution over time (insert) for the system with a tube length of 1.25 nm, a crossing angle of 20° and an initial spacing of 0.5σ.

respectively. From the profile of the middle SWNT, it can be seen that over the time length the steady-state heat transfer has already been achieved and the steady-state temperature value of the middle SWNT is about 300 K. Figure 2 shows the temperature profile of the system. As mentioned before, each SWNT is divided into 2 slabs along y direction (i.e., the transverse direction) to obtain the local temperature. Thus, both the temperature distribution of an individual CNT along transverse direction and the inter-tube temperature distribution are given in the profile. It is shown that there are significant jumps between the neighboring SWNTs while the temperatures of the 2 slabs of the middle SWNT are almost the same, which indicates that the thermal resistance of an individual CNT to heat flow along transverse direction is much smaller compared with the inter-tube resistance. It is physically reasonable since the intra-tube C-C bonded interactions are much stronger than the inter-tube van der Waals interactions. Besides, there exist two inter-tube resistances in the system of three SWNTs and in our calculations the final results are obtained by averaging them.

Meanwhile, the structure of the steady-state system as shown in Figure 2 demonstrates the nanotubes deform during the heat transfer process. The nanotubes in the left and right side bend and the middle one is squashed. In other words, for the system with an initial nanotube spacing of 0.5σ, the nanotubes depart from each other at the contact. The actual spacing at the contact becomes very close to van der Waals diameter, while that at the boundary remains the initial value as the fixed boundary condition is applied. The systems with various initial spacings are investigated in our work. It is found that in all cases the actual spacing at the contact is close to van der Waals diameter.

Based on the definition of the thermal resistance at an interface, the thermal resistance at the interfaces between the crossed SWNTs is equal to the temperature jump between neighboring SWNTs divided by the heat flux across the interface. The thermal resistances at the interfaces between crossed (5, 5) SWNTs with a tube length of 2.5 nm as a function of the crossing angle and initial tube spacing are shown in Figure 3. The results show that the resistances are of the order of 10^9–10^{11} K/W, which are of the same order of magnitude as those obtained in previous MD studies. Evans *et al.*[20] reported the thermal resistance of a 90° junction of (10, 10) CNTs with a length of 2 nm was about 2.32×10^{10} K/W. Zhong and Lukes[17] predicted the interfacial thermal resistances between 5 nm long offset parallel (10, 10) SWNTs at a comparable spacing with our work were at the range of 6–7 $\times 10^{10}$ K/W. The simulations of Maruyama *et al.*[16] showed the inter-tube thermal resistance in an (5, 5) SWNT bundle with a length of 2.51 nm was about 1.38×10^{10} K/W. Here, it is noted that in the latter two literature the resistances were calculated in unit of m^2·K/W and for comparison the values are divided by their corresponding cross-sectional areas to be converted into the same unit as our results.

Figure 3(a) shows the dependence of the thermal resistance at the interfaces between the crossed CNTs on the crossing angle with three different initial values of tube spacing. The thermal resistance increases with the crossing angle at the range of 0°–90° in all three cases and the resistances with a crossing angle of 90° are about four to five times those with a 0° crossing angle. Besides, the resistance increases with the initial tube spacing, which is presented in Figure 3(b) more clearly. As mentioned before, for the systems with

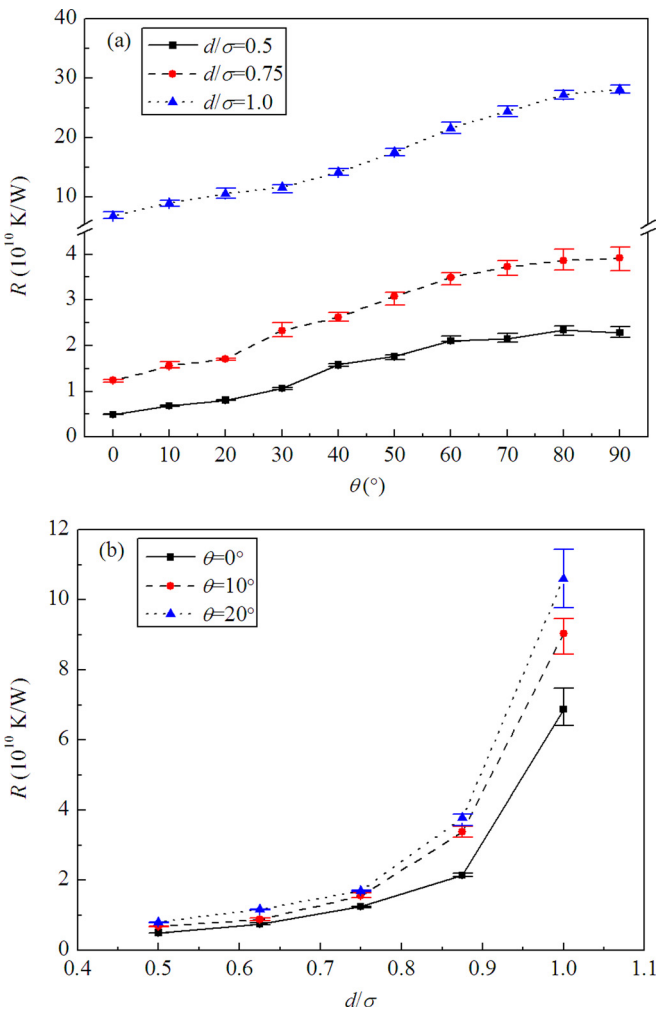

FIG. 3. Dependence of the thermal resistance at an interface between the 2.5 nm long crossed SWNTs on the (a) crossing angle and (b) initial spacing.

[This article is copyrighted as indicated in the article. Reuse of AIP content is subject to the terms at: http://scitation.aip.org/termsconditions. Downloaded to] IP: 101.6.32.33 On: Thu, 12 Dec 2013 00:34:47

various initial spacings, the actual spacings at the contact are all very close to van der Waals diameter, but those at the boundary remain the initial values considering the fixed boundary condition. Thus, the inter-tube van der Waals interactions modeled by the LJ potential that weaken with the increasing distance decrease with the increasing initial tube spacing. Besides, as the initial spacing decreases, the CNTs are getting more deformed and flatter at the contact, thus increasing the area of interaction and which in turn decreases the resistance. The increase of the thermal resistance with the initial tube spacing is dramatic at large values (around the van der Waals diameter σ). The resistance increases by an order of magnitude as the initial spacing increases from 0.5σ to 1.0σ, while it is less than double when the initial spacing is increased from 0.5σ to 0.75σ. Zhong and Lukes[17] observed the similar dramatic increase of the tube-tube thermal resistance based on their offset parallel SWNTs model. They found the resistance increased significantly at a spacing of about 0.2 nm where they set the van der Waals diameter to be 0.228 nm.

The dependence of the thermal resistance at the interfaces between the crossed CNTs on the tube length is also obtained. As shown in Figure 4, the resistance decreases with the nanotube length and converges to a constant value eventually in all our four cases with various initial tube spacings. The cases of the initial tube spacings of 0.5σ and 0.75σ can be clearly seen in the inset in Figure 4. A similar decrease for longer nanotubes was found by Zhong and Lukes[17] for the offset parallel CNT-CNT thermal resistance, while a linear decrease with the tube length was observed by Evans *et al.*[20] for the thermal resistance of a 90° junction of (10, 10) CNTs. The presence of more low-frequency phonon modes in the longer nanotubes may enable increased tube-tube coupling, leading to reduced resistance.

For some of the above results in Figures 3 and 4, overlapping error bars prevent full separation of resistance values for some of the cases of crossing angle, length, or initial spacing. However, the totality of the data suggests that there are clear reductions in thermal resistance between crossed CNTs with smaller crossing angle, longer length (before the convergence), and shorter initial spacing. The conclusion provides a clear guidance on the enhancement of the thermal conductivity of bulk CNT samples.

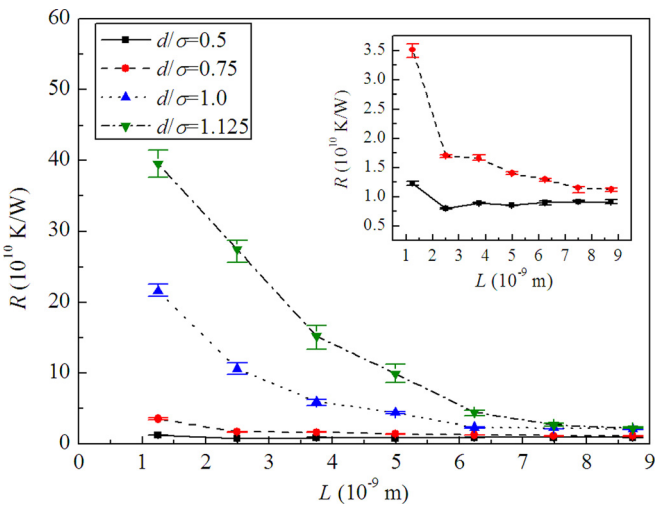

FIG. 4. Dependence of the thermal resistance at an interface between the 20° crossed SWNTs on the tube length.

B. Theoretical analyses

Between the crossed CNTs, the phonon transport is constricted through the contact and the CNT/CNT contact forms a nanometer scale constriction. In the case, all of the heat flow lines are constrained to pass through the constriction and a temperature drop can be obtained in the analytical solutions of the configuration. Constriction resistance is a measure of the additional temperature drop associated with a single constriction. Actually, a constriction resistance exists at the contact between crossed CNTs. The constriction resistance at a contact between two solid materials has been extensively studied.[30–33] There are two expressions of the constriction resistance in limiting cases. At the Maxwell's limit where the radius of the constriction (a) is much larger than the phonon mean free path (l), i.e., the Knudsen number $Kn = l/a \ll 1$, the macroscopic transport theory is valid and the diffusive constriction resistance R_{cd} is given by the Maxwell constriction resistance[30] as

$$R_{cd} = \frac{1}{2ka}, \tag{5}$$

where k is the thermal conductivity. The physical image is clear for isotropic materials. For one-dimension conductors, like CNTs, however, the physical process of thermal transport through the constriction needs to be clarified first in order to find out the physical meaning of the thermal conductivity that can be used here. For CNTs, the thermal resistance of an individual CNT to heat flow along transverse direction can be neglected as discussed before, which verifies their one-dimension structural characteristics. In the thermal transport process through the constriction, the heat flow is constrained to pass through the constriction and the contact spot of the cold CNT is heated. Then, considering the one-dimension structural characteristics of CNTs, a heat conduction process along the axial direction with a heat source occurs in the cold CNT. Therefore, the thermal conductivity along the axial direction is available in Eq. (5) and its value should be obtained in a heat conduction process with internal heat source. At the Knudsen limit of $Kn \gg 1$, the ballistic transport of phonons takes place. By integrating the ballistic phonon flux from different directions through a constriction and assuming a frequency-independent phonon group velocity (v_g), the heat flux transferred through the constriction can be obtained as

$$\dot{Q} = \frac{v_g}{4\pi} A \Delta T \sum_3 \int_0^{\omega_m} \int_0^{2\pi} \int_0^{\pi/2} \frac{\partial \langle n_0 \rangle}{\partial T} \times D(\omega) \hbar \omega \cos\theta \sin\theta \mathrm{d}\theta \mathrm{d}\varphi \mathrm{d}\omega, \tag{6}$$

where A is the area of the constriction, ω is the frequency of the phonons, ω_m is the maximum frequency of phonons, and $\langle n_0 \rangle$ is the occupation of phonons given by the Bose-Einstein distribution corresponding to the local

[This article is copyrighted as indicated in the article. Reuse of AIP content is subject to the terms at: http://scitation.aip.org/termsconditions. Downloaded to] IP: 101.6.32.33 On: Thu, 12 Dec 2013 00:34:47

equilibrium temperature T, $D(\omega)$ is the phonon density of states at frequency ω, $\hbar$ is Planck's constant, θ is the polar angle, and ϕ is the azimuthal angle. The ballistic constriction resistance R_{cb} (Ref. 31) is obtained as

$$R_{cb} = \Delta T\dot{Q} = \frac{4}{ACv_g} = \frac{4}{Cv_g\pi a^2}, \quad (7)$$

where C is the specific heat per unit volume. For one-dimension conductors, like CNTs, using $k = Cv_g l$, Eq. (7) can be written as

$$R_{cb} = \frac{4l}{kA}. \quad (8)$$

The thermal conductivity used here is also the value along the axial direction and obtained in a heat conduction process with internal heat source, In analogy to electron transport across constrictions,[32,33] a single equation for the thermal constriction resistance R_c was introduced by adding up the diffusive resistance and ballistic resistance

$$R_c = R_{cd} + R_{cb} = \frac{1}{2ka} + \frac{4l}{kA} = \frac{1}{2ka}\left(1 + \frac{8}{\pi}Kn\right). \quad (9)$$

The analytical model has been widely used to predict the thermal resistance of nanosized constrictions which can be found at nanoscale point contacts such as the nanostructure-substrate contact and the contact between a planar surface and a curved nanostructure.[34–36]

However, the analytical model of the thermal constriction resistance rests on the underlying assumption that the two objects on both sides of the constriction are the same material and same constituent phases. For the contact between crossed CNTs, the assumption fails. The combination of a poor chemical adherence at the CNT/CNT interface and a thermal expansion mismatch of the two crossed CNTs will raise the interfacial thermal resistance.[37] The interfacial resistance is due to phonon scattering at an interface. When a phonon attempts to traverse the interface, it will scatter at the interface due to the differences in vibrational properties in the crossed CNTs with the mismatch of crystal structure at the contact. Thus, it is believed that the total thermal resistance between crossed CNTs is given by the thermal constriction resistance R_c and interfacial thermal resistance R_i, leading to

$$R = R_c + R_i = R_{cd} + R_{cb} + R_i = \frac{1}{2ka}\left(1 + \frac{8}{\pi}Kn\right) + R_i. \quad (10)$$

In the case of $Kn \gg 1$, Eq. (10) is reduced to

$$R = R_c + R_i = R_{cb} + R_i = \frac{4l}{kA} + R_i. \quad (11)$$

Based on the analytical model of thermal constriction resistance, the area of the constriction formed at the contact need to be determined first. At present, the exact definition of the contact area is still an open issue for CNT/CNT contacts. Yang *et al.*[22] assumed that the area was proportional to the product of the diameters of the two tubes at cross contacts. Zhong and Lukes[17] interpreted the area as the cross-sectional area occupied by nanotubes in bundles while Varshney *et al.*[19] assumed a rectangular cross-section area with length of the CNT length and width of van der Waals contact or the nanotube diameter for aligned contacts. However, as the CNTs have deformed in our simulation the above methods are not applicable. In this paper, the constriction area at the contact between crossed CNTs is obtained from the total inter-tube van der Waals energy normalized by the reference van der Waals energy per unit area calculated for flat graphite sheets with good adherence, which is similar as that used by Evans *et al.*[20] Using this method, the value of the constriction area which is not affected by the shape of the constriction reflects the inter-tube interaction more clearly and directly. Besides, the characteristic radius of the constriction is obtained by roughly assuming a circular constriction.

Figure 5 shows the dependence of the constriction area on the crossing angle in the cases with a tube length of 2.5 nm and an initial spacing of σ, while the inset in Figure 5 gives the dependence of the thermal resistances on the inverse constriction area in those cases. It can be seen that the area decreases with the increasing crossing angle and the resistance inversely proportional to the area, which gives a good explanation of the increase of the thermal resistance with the crossing angle based on Eq. (10). The dependence of the constriction area on the tube length in the cases with a crossing angle of 20° and an initial spacing of σ is shown in Figure 6 and the corresponding thermal resistances are presented in the inset in Figure 6. The results indicate that the area increases with the tube length and converges to a constant value eventually, which partly explains the dependence of the thermal resistance on the tube length. Besides, the dependence of the area on the tube length is reasonable since the area obtained in our work increases with the projected area of the two crossed CNTs and the projected area will increase the tube length when the length is shorter than a characteristic tube length that equals to $D/\tan(\theta/2)$, where D is the diameter of

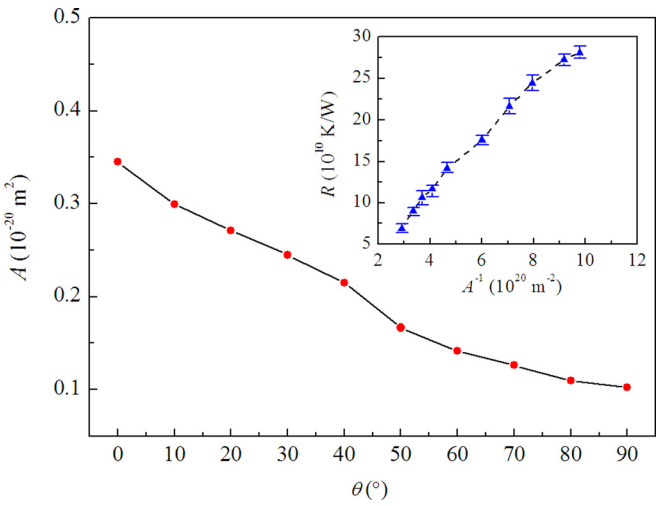

FIG. 5. Dependence of the constriction area on the crossing angle and the thermal resistance on the inverse constriction area (insert) for the systems with a tube length of 2.5 nm and an initial spacing of σ.

[This article is copyrighted as indicated in the article. Reuse of AIP content is subject to the terms at: http://scitation.aip.org/termsconditions. Downloaded to] IP: 101.6.32.33 On: Thu, 12 Dec 2013 00:34:47

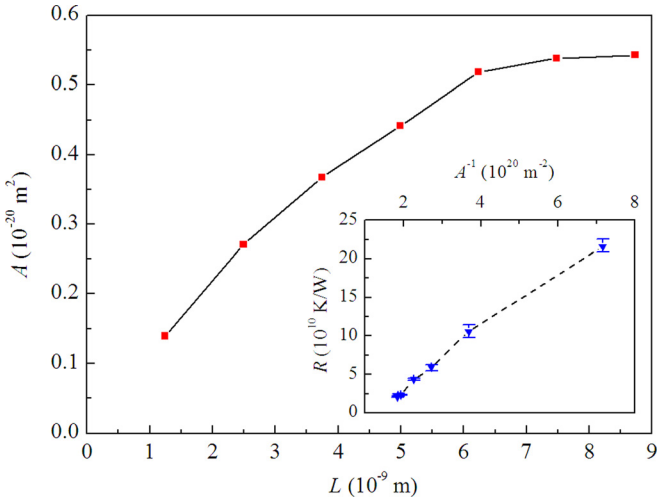

FIG. 6. Dependence of the constriction area on the tube length and the thermal resistance on the inverse constriction area (insert) for the systems with a crossing angle of 20° and an initial spacing of σ.

the tube and θ is the crossing angle and converge to a constant value when the length is larger than it.

The above discussion about the thermal resistance between crossed SWNTs is qualitative. As to confirm the application of the analytical model of thermal constriction resistance in the thermal resistance between crossed SWNTs, the quantitative comparison is necessary. In our previous work, the thermal conductivities of (5, 5) SWNTs with internal heat source have been obtained, as shown in Figure 7. The value for 2.5 nm long (5, 5) SWNT is about 15 W/(m K). The specific heat C is obtained by converting the results obtained for SWNT ropes[38] using the density of graphite. Using a typical v_g of about 10^4 m/s for the four acoustic modes of a (5, 5) SWNT,[39,40] we obtain that the phonon mean free path l is about 0.623 nm. Based on Matthiessen's rule, considering Umklapp phonon scattering and phonon-boundary scattering the phonon mean free path can be expressed as $l^{-1} = l_U{}^{-1} + c_M L^{-1}$, where l_U is the phonon mean free path due to Umklapp scattering, L is the length of the CNT, c_M is a constant. Figure 7 also shows the linear fitting of the MD results and the theoretical values based on the

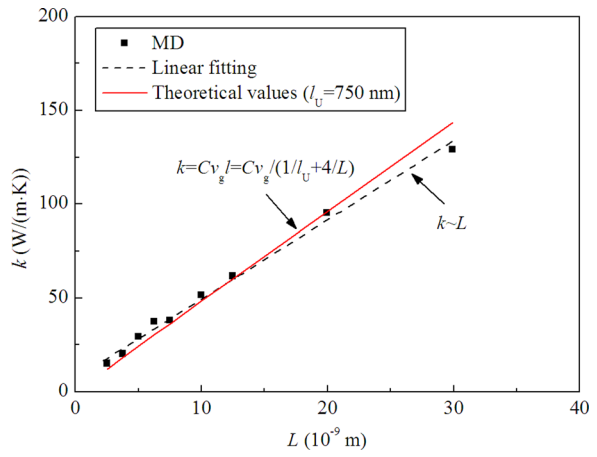

FIG. 7. Dependence of the thermal conductivity of (5, 5) SWNT on the tube length.

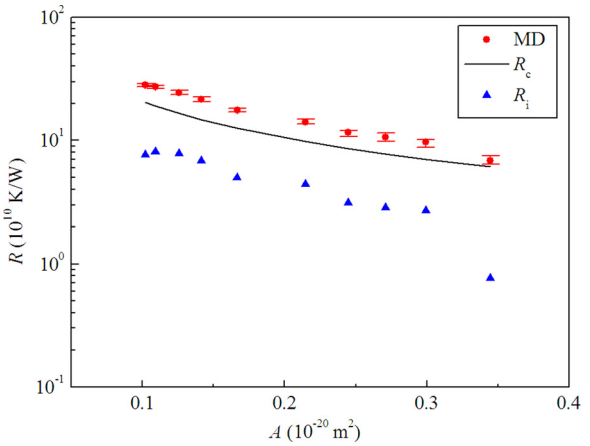

FIG. 8. Dependence of the thermal resistance at an interface between the crossed SWNTs calculated by MD on the contact area with comparison to the theoretical predictions of the thermal constriction resistance and interfacial thermal resistance.

above phonon mean free path formula. It is obtained that l_U is about 750 nm that is consistent with the results in Ref. 41 and the thermal conductivity is proportional to the tube length in our studied range. Besides, the phonon-boundary scattering is the main cause of the quite small value of the phonon mean free path. As the fixed boundary condition is applied in the axial direction of the CNT, the effective length for energy transmission (L_e) is shorter than the length of the CNT. Meanwhile, in the SWNTs with internal heat source, the phonon mean free path is about half of the effective length for energy transmission since the energy transmission distance of the phonon at a position x is x and L_e-x in the left and right direction, respectively.

Based on the phonon mean free path and constriction area obtained before, the Knudsen number is predicted to be much greater than one. The ballistic constriction resistance will be much larger than the diffusive constriction resistance. Then, the analytical values of thermal constriction resistance can be obtained based on Eq. (8). Figure 8 presents the values of the calculated thermal resistances in the cases with an initial tube spacing of σ, a length of 2.5 nm and various crossing angles, the thermal constriction resistance R_c, and the interfacial thermal resistance R_i obtained by subtracting R_c from the calculated thermal resistance based on Eq. (11). It can be seen the thermal constriction resistance is much greater than the interfacial thermal resistance and the thermal resistance calculated by MD is close to the constriction resistance, i.e., the ballistic constriction resistance. These findings suggest that the thermal resistance is dominated by the thermal constriction resistance and the ballistic transport of phonons is dominant in the interfacial heat transfer. Besides, since the thermal constriction resistance is given by the ballistic constriction resistance which doesn't depend on the shape of the constriction,[35] the error of the obtained radius due to the non-circular constriction shape does not affect our results.

IV. CONCLUSIONS

Systems of crossed (5, 5) SWNTs with various crossing angles, initial nanotube spacings, and nanotube lengths are

[This article is copyrighted as indicated in the article. Reuse of AIP content is subject to the terms at: http://scitation.aip.org/termsconditions. Downloaded to] IP: 101.6.32.33 On: Thu, 12 Dec 2013 00:34:47

constructed and the thermal resistance between the crossed CNTs is investigated by using MD simulations. The results show that the thermal resistance is of the order of 10^9–10^{11} K/W. Besides, the thermal resistance increases with the increasing crossing angle and initial nanotube spacing while decreases with the increasing nanotube length and converges to a constant eventually. These findings indicate that good orientation may decrease the thermal resistance between crossed CNTs and enhance their thermal conductance, which is also applicable to other low-dimensional structures, such as polymer nanowires.[42,43] Since heat is constricted to flow through the contact between the crossed CNTs, a thermal constriction resistance exists at the contact. Meanwhile, an interfacial thermal resistance is induced by the poor chemical adherence and thermal expansion mismatch at the CNT/CNT interfaces. Thus, the total thermal resistance at a CNT/CNT contact is given by the thermal constriction resistance and interfacial thermal resistance. Based on the analytical model of the thermal resistance, the increase of the thermal resistance with the increasing crossing angle is well explained. Our research shows that the total inter-tube thermal resistance is dominated by the thermal constriction resistance and the ballistic transport of phonons is dominant in the interfacial heat transfer between the crossed CNTs.

ACKNOWLEDGMENTS

This work was financially supported by National Natural Science Foundation of China (Nos. 51322603, 51136001, 51321002), Program for New Century Excellent Talents in University, and Tsinghua University Initiative Scientific Research Program.

[1]E. Pop, D. Mann, Q. Wang, K. Goodson, and H. Dai, Nano Lett. **6**, 96 (2006).
[2]S. Berber, Y. K. Kwon, and D. Tomanek, Phys. Rev. Lett. **84**, 4613 (2000).
[3]M. Fujii, X. Zhang, H. Q. Xie, H. Ago, K. Takahashi, T. Ikuta, H. Abe, and T. Shimizu, Phys. Rev. Lett. **95**, 065502 (2005).
[4]G. J. Hu and B. Y. Cao, Mol. Simul. **38**, 823 (2012).
[5]M. J. Biercuk, M. C. Llaguno, M. Radosavljevic, J. K. Hyun, A. T. Johnsond, and J. E. Fischer, Appl. Phys. Lett. **80**, 2767 (2002).
[6]I. Alexandrou, E. Kymakis, and G. A. J. Amaratunga, Appl. Phys. Lett. **80**, 1435 (2002).
[7]S. U. S. Choi, Z. G. Zhang, W. Yu, E. A. Lockwood, and E. A. Grulke, Appl. Phys. Lett. **79**, 2252 (2001).
[8]J. A. Eastman, S. R. Phillpot, S. U. S. Choi, and P. Keblinski, Annu. Rev. Mater. Res. **34**, 219 (2004).
[9]S. Ujereh, T. Fisher, and I. Mudawar, Int. J. Heat Mass Transfer **50**, 4023 (2007).
[10]S. Shenogin, L. P. Xue, R. Ozisik, P. Keblinski, and D. G. Cahill, J. Appl. Phys. **95**, 8136 (2004).
[11]S. T. Huxtable, D. G. Cahill, S. Shenogin, L. P. Xue, R. Ozisik, P. Barone, M. Usrey, M. S. Strano, G. Siddons, M. Shim, and P. Keblinski, Nature Mater. **2**, 731 (2003).
[12]A. K. Vallabhaneni, B. Qiu, J. N. Hu, Y. P. Chen, A. K. Roy, and X. L. Ruan, J. Appl. Phys. **113**, 064311 (2013).
[13]J. Hone, M. C. Llaguno, N. M. Nemes, A. T. Johnson, J. E. Fischer, D. A. Walters, M. J. Casavant, J. Schmidt, and R. E. Smalley, Appl. Phys. Lett. **77**, 666 (2000).
[14]A. E. Aliev, M. H. Lima, E. M. Silverman, and R. H. Baughman, Nanotechnology **21**, 035709 (2010).
[15]P. L. Kapitza, J. Phys. (USSR) **4**, 181 (1941).
[16]S. Maruyama, Y. Igarashi, Y. Taniguchi, and J. Shiomi, J. Therm. Sci. Technol. **1**, 138 (2006).
[17]H. Zhong and J. R. Lukes, Phys. Rev. B **74**, 125403 (2006).
[18]Z. Xu and M. J. Buehler, ACS Nano **3**, 2767 (2009).
[19]V. Varshney, S. S. Patnaik, A. K. Roy, and B. L. Farmer, J. Phys. Chem. C **114**, 16223 (2010).
[20]W. J. Evans, M. Shen, and P. Keblinski, Appl. Phys. Lett. **100**, 261908 (2012).
[21]B. A. Cola, J. Xu, and T. S. Fisher, Int. J. Heat Mass Transfer **52**, 3490 (2009).
[22]J. Yang, S. Waltermire, Y. Chen, A. A. Zinn, T. T. Xu, and D. Li, Appl. Phys. Lett. **96**, 023109 (2010).
[23]W. G. Hoover, Annu. Rev. Phys. Chem. **34**, 103 (1983).
[24]D. S. Portal, E. Artacho, J. M. Soler, A. Rubio, and P. Ordejon, Phys. Rev. B **59**, 12678 (1999).
[25]S. Nose, Mol. Phys. **52**, 255 (1984).
[26]W. G. Hoover, Phys. Rev. A **31**, 1695 (1985).
[27]D. J. Evans and B. L. Holian, J. Chem. Phys. **83**, 4069 (1985).
[28]D. W. Brenner, Phys. Rev. B **42**, 9458 (1990).
[29]R. Saito, R. Matsuo, T. Kimura, G. Dresselhaus, and M. S. Dresselhaus, Chem. Phys. Lett. **348**, 187 (2001).
[30]M. G. Cooper, B. B. Mikic, and M. M. Yovanovish, Int. J. Heat Mass Transfer **12**, 279 (1969).
[31]E. T. Swartz and R. O. Pohl, Rev. Mod. Phys. **61**, 605 (1989).
[32]B. Nikolic and P. B. Allen, Phys. Rev. B **60**, 3963 (1999).
[33]M. J. M. de Jong, Phys. Rev. B **49**, 7778 (1994).
[34]L. Weber, E. Gmelin, and H. J. Queisser, Phys. Rev. B **40**, 1244 (1989).
[35]R. Prasher, Nano Lett. **5**, 2155 (2005).
[36]S. K. Saha and L. Shi, J. Appl. Phys. **101**, 074304 (2007).
[37]C. W. Nan, R. Birringer, D. R. Clarke, and H. Gleiter, J. Appl. Phys. **81**, 6692 (1997).
[38]J. Hone, B. Batlogg, Z. Benes, A. T. Johnson, and J. E. Fischer, Science **289**, 1730 (2000).
[39]M. S. Dresselhaus and P. C. Eklund, Adv. Phys. **49**, 705 (2000).
[40]Q. W. Hou, B. Y. Cao, and Z. Y. Guo, Acta Phys. Sin. **58**, 7809 (2009) (in Chinese).
[41]S. Ghosh, I. Calizo, D. Teweldebrhan, E. P. Pokatilov, D. L. Nika, A. A. Balandin, W. Bao, F. Miao, and C. N. Lau, Appl. Phys. Lett. **92**, 151911 (2008).
[42]B. Y. Cao, Y. W. Li, J. Kong, H. Chen, Y. Xu, K. L.Yung, and A. Cai, Polymer **52**, 1711 (2011).
[43]B. Y. Cao, J. Kong, Y. Xu, K. L.Yung, and A. Cai, Heat Transfer Eng. **34**, 131 (2013).

[This article is copyrighted as indicated in the article. Reuse of AIP content is subject to the terms at: http://scitation.aip.org/termsconditions. Downloaded to] IP: 101.6.32.33 On: Thu, 12 Dec 2013 00:34:47